

# Synthesis and Characterization of Selected Metal Oxide Nanoparticles

Jitesh Rami<sup>1\*</sup>, Chirag Patel<sup>2</sup>, Mansish Patel<sup>3</sup>

Assistant Teacher Sanesada<sup>1</sup>

Associate Professor, Sankalchand Patel college of Engineering, Sankalchand Patel University, Visnagar,  
Gujarat 384315, India <sup>2&3</sup>

jr17792@gmail.com<sup>\*1</sup>, chiragkansa@gmail.com<sup>2</sup>, mvpatelphy@gmail.com<sup>3</sup>

**Abstract:** In the present study, oxide nanoparticles of copper, cobalt, iron and zinc metals have been synthesized using a chemical co-precipitation approach. This gives a large scale production of metal oxide nanoparticles. The structural properties of the synthesized metal oxide nanoparticles were studied using X-ray diffraction (XRD). The XRD result reveals the crystalline nature of the metal oxide nanoparticles. Additional, scanning electron microscopy (SEM) was also performed to study the morphology of the selected four metal oxide nanoparticles. SEM micrograph showed the spherical morphology of as prepared CuO, CO<sub>2</sub>O<sub>3</sub>, Fe<sub>2</sub>O<sub>3</sub> and ZnO nanoparticles also they are interspersed with each other.

**Keywords:** Chemical co-precipitation, Metal oxide nanoparticles, SEM, XRD

## I. INTRODUCTION

An important class of semiconductors called transition metal oxides finds use in magnetic-storage, solar-energy conversion, electronics, and catalysis [1-4]. In an effort to improve the purity of the synthesized product and characterize it using various techniques, researchers have tried to synthesise various nanoparticles using various ways in an effort to obtain inexpensive, simple processes that take less time and effort. Due to their effectiveness as nanofluids in applications involving heat-transfer, copper oxide nanoparticles are of particular interest among the transition metal oxides. For instance, it has been observed that adding 4 percent CuO increases water's thermal conductivity by more than 20 percent [5-9]. CuO is a semiconducting material with a fine band gap that is employed in photothermic and photo conductive applications [10]. Cobalt oxide nanoparticles have been exploited in catalysis, capacitors, magnetoresistance materials, sensors, energy storage system electrode, and FETs, and [11-16]. Cobalt oxide has received attention as a supercapacitor and battery contender in recent years. Cobalt oxide enhanced the electrode's capacitance in a supercapacitor electrode that used carbon nanotubes and CO<sub>2</sub>O<sub>3</sub> nanocomposite [17, 18]. Iron oxide nanoparticles are of great interest for a variety of technological applications, including high-density magnetic recording media, sensors, catalysts, and medical uses. This interest stems from iron oxide nanoparticles' multivalent oxidation states, abundant polymorphism, and mutually polymorphous changes in nanophase [19-25]. At ambient temperature, zinc oxide (ZnO) has an energy gap of 3.37 eV. It has been widely employed due to its catalytic, electrical, optoelectronic and photochemical characteristics [26, 27]. Because of its enormous surface area and strong catalytic activity, ZnO nanostructures are ideal for use in catalytic reaction processes [28]. Because zinc oxide has varying physical and chemical characteristics depending on the morphology of nanostructures, not only are different synthesis techniques to be researched, but also the physical and chemical properties of generated zinc oxide in terms of its morphology.

In the present work, a chemical co-precipitation method is used to synthesize the metal oxide nanoparticles. The metal oxide nanoparticles were further rectified for its structural purity by XRD and also analyzed by Scanning Electron Microscope (SEM) for their morphology.

## II. METHODS AND MATERIALS

### A. Chemicals

All chemicals used in the experiment are analytic reagent grade and are used lacking advance purification. Freshly formulated aqueous solutions of chemicals are used for nanoparticle separation. Metal oxide solution and ethylenediaminetetraacetic (EDTA) acid were collected from Department of Chemistry, HNGU, Patan, Gujarat, India. Sodium hydroxide NaOH (pellets) was collected from Physics Department, Sheth M.N. Science College, Patan, Gujarat, India. Deionized water was used for the preparation of solutions.

### B.Synthesis

Oxide nanoparticles of Copper, Cobalt, Iron and Zinc are prepared by dropping simultaneously 60 ml of 0.4 M solution of Metal oxide into 60 ml of 0.0125 M solution of ethylene-diamine-tetra-acetic acid which is vigorously stirred using a magnetic-stirrer. The role of EDTA was to stabilize the particles next to aggregation, which may shepherd the particle to nano size. The metal-carbonate precipitate formed by this reaction is separated from the reaction mixture and washed several times with filtered water and then with alcohol to remove contaminations, including EDTA waste, and to eliminate any original reactant. The wet precipitate is dehydrated and meticulously pulverized using an agate-mortar to get metal-carbonate precursor in the form of extremely fine powder. At high temperatures, the metal-carbonate precursor transforms into metal oxide nanoparticles.

### C.Characterization

The structural study of oxide nanoparticles of copper, cobalt, iron and zinc samples was carried out by X-ray diffraction (XRD) plots illustrated with a Bruker, D2 Phaser X-ray Diffractometer (with  $\text{CuK}\alpha$  radiation) in the range  $10^\circ$  to  $90^\circ$ . Morphological studies of the materials were done with the Scanning Electron Microscope (SEM, Jeol, JSM6010LA). The average crystallite size ( $t$ ) has been calculated from the line broadening using Scherrer's relation:

$$t = 0.9\lambda/\beta\cos\theta \quad (1)$$

Where,  $D$  is the average crystalline size,  $\lambda$  is the wavelength of X-ray and  $\beta$  is peak width of half maximum (FWHM).

## III.RESULT AND DISCUSSION

### A. XRD Analysis

The middling crystallite size was measured by Debye-Scherer's equation using the help of XRD configurations as shown in Figure 1(a, b, c, d). For CuO nanoparticles, crisp and strong peak found at approx  $35^\circ$  and  $38^\circ$  positions with (1 1 1) and (0 2 2) respectively indicates that the sample has high crystalline quality and is in the monoclinic structure with lattice parameters, and which is in good accord with JCPDS card number 45-0937 [29]. The peak positions and some of the (h, k, l) values have bars at the top, which indicates that the associated peak is moving in the opposite direction (h, k, l). The fact that all of the peaks are extremely sharp and that there are no crystallinity imperfections indicates that the sample is highly pure.

The XRD pattern of  $\text{Co}_2\text{O}_3$  nanoparticles shown in Fig. 1(b). It does not display any peaks for the sample as it was originally created, confirming that the technique is necessary to maintain the crystalline phase and avoid their agglomeration. The nanoparticles of  $\text{Co}_2\text{O}_3$  sample shows peak intensities of (1 1 0), (2 2 0), (3 1 1), (4 0 0), (4 2 2), (5 1 1) and (4 4 0) reveal the  $\text{Co}_2\text{O}_3$  with cubic phase (space group:  $\text{Fd}3\text{m}$ ). Overall, the supplementary negligible peaks are existing in the primed sample due to contamination. The acquired XRD peaks match those of JCPDS card no. 76-1802 and are coordinated with the  $\text{Co}_2\text{O}_3$  standard characteristic peaks [30].

The XRD pattern of prepared  $\text{Fe}_2\text{O}_3$  nanoparticles is presented in Fig. 1(c). The most intense peak was observed at  $\sim 35.5^\circ$ . The diffraction peaks seemed at different angles supported with the JCPDS-86-0550 values, which can be associated with the (0 1 2), (1 0 4), (1 1 0), (1 1 3), (0 2 4), (1 1 6), (0 1 8), (2 1 4) and (3 0 0) planes of  $\alpha\text{-Fe}_2\text{O}_3$ . This demonstrated that the final particles were pure  $\alpha\text{-Fe}_2\text{O}_3$  and free of any additional contaminants or iron oxide phases. The broad breadth of the diffraction pattern suggests that the particles are smaller in size [31].

The XRD peaks of nanoparticles of ZnO sample shown in Fig.1(d), the XRD patterns with lattice parameter of  $a$  and  $c$  were suggest the pure hexagonal structure and space group:  $\text{P}63\text{mc}$  of ZnO nanoparticles. The peaks appeared (1 0 0), (0 0 2), (1 0 1), (1 0 2), (1 1 0), (1 0 3), (1 1 2) values relate to pure ZnO. They are alike with the standard JCPDS card no.01- 79-0206, showing that ZnO particles are crystalline structure [32].

The average crystalline size of all four metal oxide nanoparticles was attained between 30-50 nm which is calculated using Debye-Scherer's equation.

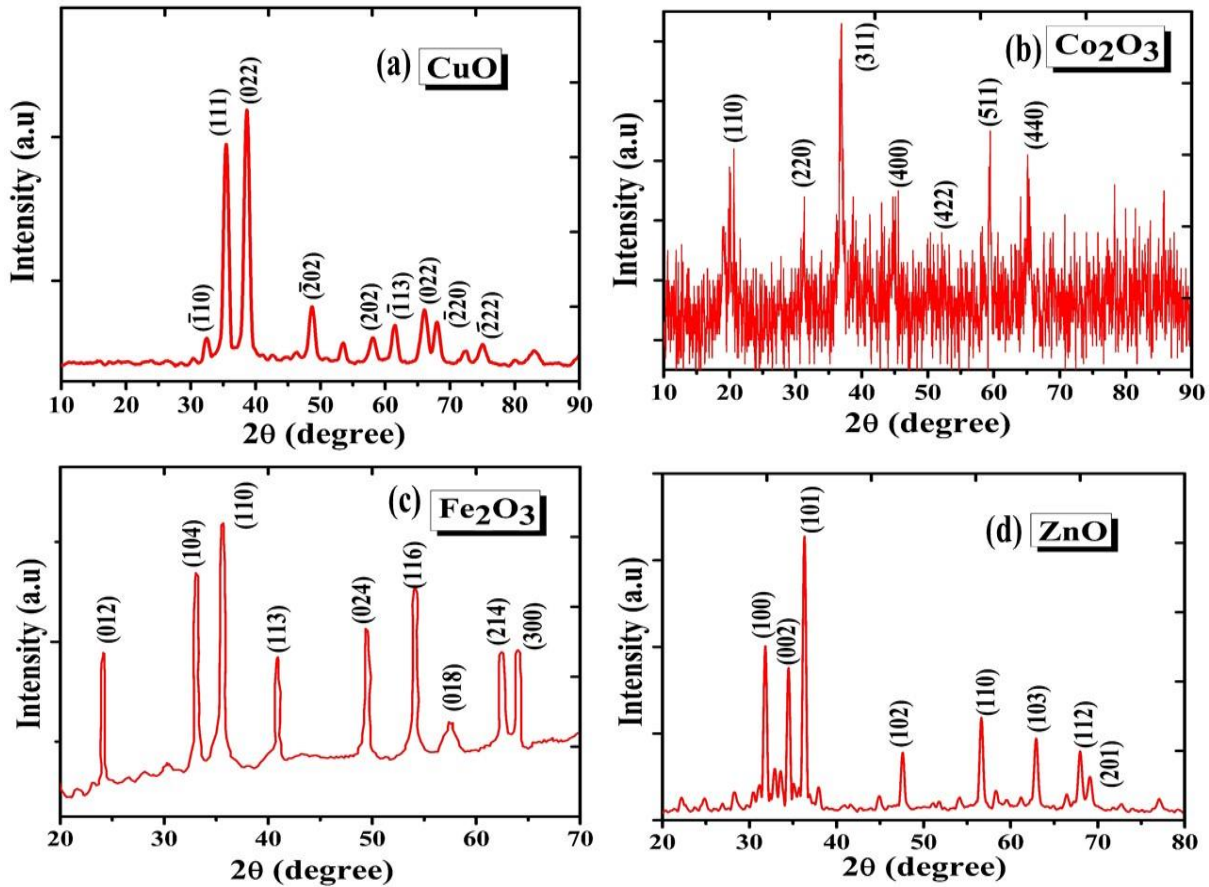
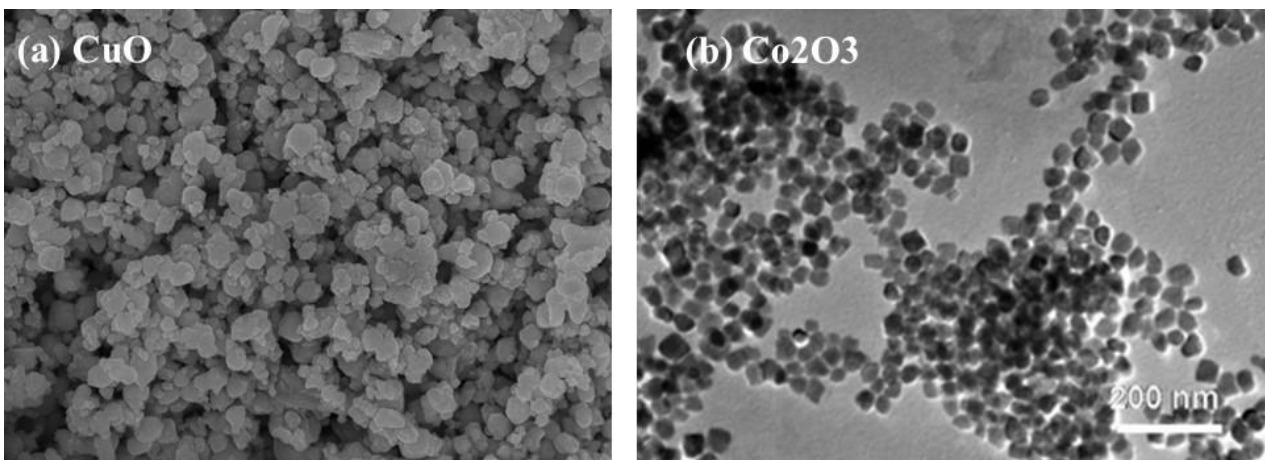


Fig.1XRD of (a) Copper Oxide, (b) Cobalt Oxide, (c) Iron Oxide and (d) Zinc Oxide Nanoparticles

**B. SEM Analysis**

The morphology of the synthesized metal oxide nanoparticles shows in Fig. 2 (a, b, c, d). SEM image shows a sphere like morphology of all the metal oxide nanoparticles and it contains agglomerated accumulated particles indicating good connectivity between the nanoparticles. The size of nanoparticles, their homogeneity, and their size distribution are revealed by SEM. The SEM image shows that the distribution of the particles is uniform. In cobalt oxide nanoparticles, this morphology is favorable to manufacture the electrode for super-capacitor application because of a material with high surface area [33]. We have observed variation in all four metal oxide nanoparticles size from 35 nm to 200 nm. The measured particle size is bigger than what has been documented in the literature. The fact that the particles were grouped together may have contributed to the larger nanoparticle sizes in the current study.



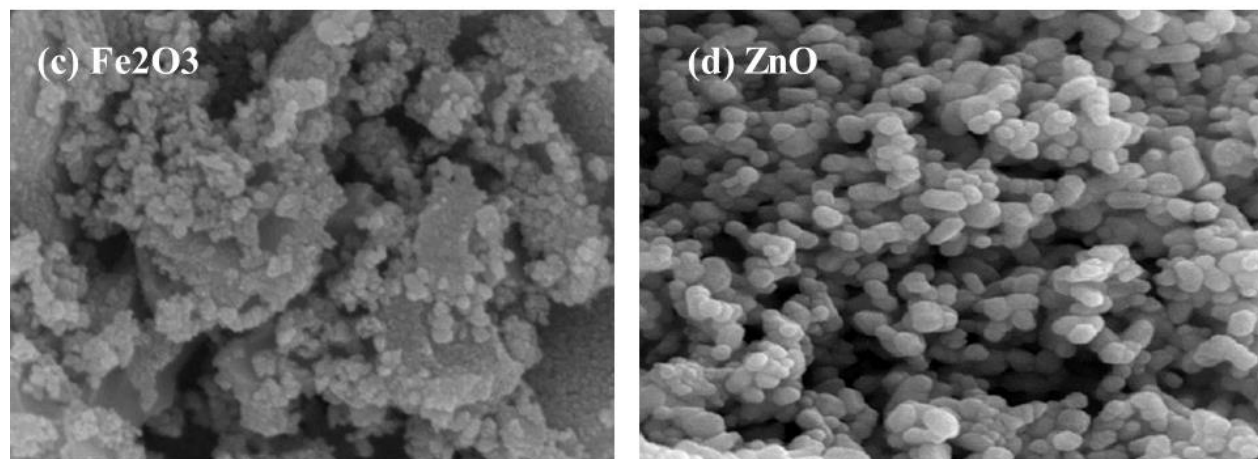


Fig.2 SEM micrograph of (a) Copper Oxide, (b) Cobalt Oxide, (c) Iron Oxide and (d) Zinc Oxide Nanoparticles

#### IV. CONCLUSION

Synthesis of CuO, Co<sub>2</sub>O<sub>3</sub>, Fe<sub>2</sub>O<sub>3</sub> and ZnO nanoparticles with chemical co-precipitation method has been carried out commendably. We found distinct peaks in the XRD patterns of all four samples of metal oxide nanoparticles, proving that they were naturally crystalline and average crystalline size is between 35-50 nm. SEM micrographs were used to analyse the nanoparticles' morphology. The nanoparticle size distribution was originating in the range of 35–200 nm. The average particle size of collected metal oxide nanoparticles was determined to be 35-55 nm.

#### REFERENCES

- [1] O'Regan, B., Graetzel, M. and Fitzmaurice, D., 1991. Optical electrochemistry. 2. Real-time spectroscopy of conduction band electrons in a metal oxide semiconductor electrode. *The Journal of physical chemistry*, 95(26), pp.10525-10528.
- [2] Zhang, Q., Park, K., Xi, J., Myers, D. and Cao, G., 2011. Recent Progress in Dye-Sensitized Solar Cells Using Nanocrystallite Aggregates. *Advanced Energy Materials*, 1(6), pp.988-1001.
- [3] Bjoerksten, U., Moser, J. and Graetzel, M., 1994. Photoelectrochemical studies on nanocrystalline hematite films. *Chemistry of materials*, 6(6), pp.858-863.
- [4] Dow, W.P. and Huang, T.J., 1996. Ytria-stabilized zirconia supported copper oxide catalyst: II. Effect of oxygen vacancy of support on catalytic activity for CO oxidation. *Journal of Catalysis*, 160(2), pp.171-182.
- [5] Larsson, P.O., Andersson, A., Wallenberg, L.R. and Svensson, B., 1996. Combustion of CO and toluene; characterisation of copper oxide supported on titania and activity comparisons with supported cobalt, iron, and manganese oxide. *Journal of Catalysis*, 163(2), pp.279-293.
- [6] Jiang, Y., Decker, S., Mohs, C. and Klabunde, K.J., 1998. Catalytic solid state reactions on the surface of nanoscale metal oxide particles. *Journal of Catalysis*, 180(1), pp.24-35.
- [7] Mitsuyu, T., Yamazaki, O., Ohji, K. and Wasa, K., 1982. Piezoelectric thin films of zinc oxide for saw devices. *Ferroelectrics*, 42(1), pp.233-240.
- [8] Wohlfarth, E.P. ed., 1986. *Handbook of magnetic materials* (Vol. 2). Elsevier.
- [9] Lee, S., Choi, S.S., Li, S.A. and Eastman, J.A., 1999. Measuring thermal conductivity of fluids containing oxide nanoparticles.
- [10] Rakhshani, A.E., 1986. Preparation, characteristics and photovoltaic properties of cuprous oxide—a review. *Solid-State Electronics*, 29(1), pp.7-17.
- [11] Jagtap, S.V., Tale, A.S. and Thakre, S.D., 2017. Synthesis by sol gel method and characterization of Co<sub>3</sub>O<sub>4</sub> nanoparticles. *Int. J. Res. Eng. Appl. Sci*, 7, pp.1-6.
- [12] Salavati-Niasari, M., Khansari, A. and Davar, F., 2009. Synthesis and characterization of cobalt oxide nanoparticles by thermal treatment process. *Inorganica Chimica Acta*, 362(14), pp.4937-4942.
- [13] Rahimi-Nasrabadi, M., Naderi, H.R., Karimi, M.S., Ahmadi, F. and Pourmortazavi, S.M., 2017. Cobalt carbonate and cobalt oxide nanoparticles synthesis, characterization and supercapacitive evaluation. *Journal of Materials Science: Materials in Electronics*, 28(2), pp.1877-1888.
- [14] Wadekar, K.F., Nemade, K.R. and Waghuley, S.A., 2017. Chemical synthesis of cobalt oxide (Co<sub>3</sub>O<sub>4</sub>) nanoparticles using Co-precipitation method. *Res J Chem Sci*, 7(1), pp.53-55.

- [15] Li, W.Y., Xu, L.N. and Chen, J., 2005. Co<sub>3</sub>O<sub>4</sub> nanomaterials in lithium-ion batteries and gas sensors. *Advanced Functional Materials*, 15(5), pp.851-857.
- [16] Xie, X. and Shen, W., 2009. Morphology control of cobalt oxide nanocrystals for promoting their catalytic performance. *Nanoscale*, 1(1), pp.50-60.
- [17] Kumar, N., Yu, Y.C., Lu, Y.H. and Tseng, T.Y., 2016. Fabrication of carbon nanotube/cobalt oxide nanocomposites via electrophoretic deposition for supercapacitor electrodes. *Journal of materials science*, 51(5), pp.2320-2329.
- [18] Durukan, M.B., Yuksel, R. and Unalan, H.E., 2016. Cobalt oxide nanoflakes on single walled carbon nanotube thin films for supercapacitor electrodes. *Electrochimica Acta*, 222, pp.1475-1482.
- [19] Cornell, R.M. and Schwertmann, U., 2003. *The iron oxides: structure, properties, reactions, occurrences, and uses* (Vol. 664). Weinheim: Wiley-vch.
- [20] Cullity, B.D., 1972. *Introduction to magnetic materials*, Addison-Wesley Publishing Co. Inc. Reading MA.
- [21] Häfeli, U., Schütt, W., Teller, J. and Zborowski, M. eds., 2013. *Scientific and clinical applications of magnetic carriers*. Springer Science & Business Media.
- [22] Jiang, J.Z., Lin, R., Lin, W., Nielsen, K., Mørup, S., Dam-Johansen, K. and Clasen, R., 1997. Gas-sensitive properties and structure of nanostructured (-materials prepared by mechanical alloying. *Journal of Physics D: Applied Physics*, 30(10), p.1459.
- [23] Benz, M., Van der Kraan, A.M. and Prins, R., 1998. Reduction of aromatic nitrocompounds with hydrazine hydrate in the presence of an iron oxide hydroxide catalyst: II. Activity, X-ray diffraction and Mössbauer study of the iron oxide hydroxide catalyst. *Applied Catalysis A: General*, 172(1), pp.149-157.
- [24] Brida, D., Fortunato, E., Águas, H., Silva, V., Marques, A., Pereira, L., Ferreira, I. and Martins, R., 2002. New insights on large area flexible position sensitive detectors. *Journal of non-crystalline solids*, 299, pp.1272-1276.
- [25] Wang, Z.L., 2004. Zinc oxide nanostructures: growth, properties and applications. *Journal of physics: condensed matter*, 16(25), p.R829.
- [26] Suche, M., Christoulakis, S., Moschovis, K., Katsarakis, N. and Kiriakidis, G., 2006. ZnO transparent thin films for gas sensor applications. *Thin solid films*, 515(2), pp.551-554.
- [27] Ashour, A., Kaid, M.A., El-Sayed, N.Z. and Ibrahim, A.A., 2006. Physical properties of ZnO thin films deposited by spray pyrolysis technique. *Applied Surface Science*, 252(22), pp.7844-7848.
- [28] Chen, J.C. and Tang, C.T., 2007. Preparation and application of granular ZnO/Al<sub>2</sub>O<sub>3</sub> catalyst for the removal of hazardous trichloroethylene. *Journal of hazardous materials*, 142(1-2), pp.88-96.
- [29] Ashok, C.H., Rao, K.V. and Chakra, C.S., 2014. Structural analysis of CuO nanomaterials prepared by novel microwave assisted method. *Journal of Atoms and Molecules*, 4(5), pp.803-806.
- [30] Sharifi, S.L., Shakur, H.R., Mirzaei, A. and Hosseini, M.H., 2013. Characterization of cobalt oxide Co<sub>3</sub>O<sub>4</sub> nanoparticles prepared by various methods: effect of calcination temperatures on size, dimension and catalytic decomposition of hydrogen peroxide. *International Journal of Nanoscience and Nanotechnology*, 9(1), pp.51-58.
- [31] Ma, M., Zhang, Y., Yu, W., Shen, H.Y., Zhang, H.Q. and Gu, N., 2003. Preparation and characterization of magnetite nanoparticles coated by amino silane. *Colloids and Surfaces A: physicochemical and engineering aspects*, 212(2-3), pp.219-226.
- [32] Kumar, M., Kumar, S., Parveen, Z., Kaur, J., Sharma, N. and Bansod, B.S., 2015. Facial synthesis of nano Sized ZnO by hydrothermal method. *International Journal of Advanced Research in Electrical, Electronics and Instrumentation Engineering*, 4(5), pp.4440-4444.
- [33] Kumar, N., Sahoo, P.K. and Panda, H.S., 2017. Tuning the electro-chemical properties by selectively substituting transition metals on carbon in Ni/Co oxide-carbon composite electrodes for supercapacitor devices. *New Journal of Chemistry*, 41(9), pp.3562-3573.